RESEARCH ARTICLE OPEN ACCESS

Hybrid Technology Solar Thermal Membrane Desalination of Salt Water for Populations In The Saloum River Delta

M. Sene [a], Y. Mandiang [a], D. Azilinon [a]
Laboratoire d'Energétique Appliquée (LEA), Ecole Supérieure Polytechnique (ESP) de Dakar, BP 5085
Université Cheikh Anta Diop (UCAD) de Dakar, Senegal

Abstracts
The use of brackish water in the Saloum Delta in Senegal can be made by combining the processes of desalination as a source of solar energy, usually thermal and photovoltaic processes for membrane distillation. But the demand for energy is growing; the use of solar energy can be a good solution, given the high solar potential in these areas.
Different experiences around the world have shown that the process AGMD (Air Gap Membrane Distillation) is properly adapted to renewable energy. Our work has shown that the production of fresh water by a hybrid method of desalination is possible. Then we analyzed the results on the effect of the pore size of the membrane on the mechanisms of mass transfer to estimate the production of fresh water per day generated. We also showed the effect of hot water heated by a solar panel on the phenomena of polarization membrane solution. And the final result allowed us to estimate in a dynamic system and for a small model, a daily production of about 4 L / h.
Keyword: Solar-Desalination-Membrane distillation - production flow-dynamic system-hybrid method–brackish water

I. INTRODUCTION

The method for membrane distillation is an emerging technique for hybrid desalination, for using the difference in water vapour pressure across the membrane and whose operating range is from 40 °C to 90 °C.
In the Saloum River Delta (area of 234 000 ha, of which 40 % of mangrove swamp), 30 % of free water available is salty and strong concentration. Salinity is increasing because the Saloum river delta estuary is "reverse", despite having numerous channels. Taking into account the growing need for fresh water and salt water availability in these islands, we thought that desalination could be a must. With very large solar field, a hybrid membrane system distiller could agree for these regions, all the more since their design does not present technical difficulties. And advantages are: low operating pressures and temperatures, 100 % removal of ions and colloids [**1**], strong discharges impurities resistant membranes, low consumption energy, ability to reuse the recovered energy, etc. preprocessing unnecessary. Membrane processes (AGMD, DCMD, VMD and ADMS) are often under or poorly used. [**2**] Many advanced earlier works have been carried out [**3**] and their experimental results were found to enhance these processes. Membrane techniques, depending on the size of the available energy, such as thermal or reverse osmosis, distillation or flash successive expansions arrive daily to produce large quantities of fresh water. The global production, for these processes, was estimated to about $25\%10^6 m^3/d$ [**4**]. The Gulf countries are almost completely dependent on desalination, since 2002, 93 % of drinking water came from desalination plants [4]. The problem of reducing the energy consumption of desalination processes is becoming obvious more and more. For this end, projects for research and development [**1, 2,3,4,5** ...] were on the increase in order to improve the performance of existing techniques, in order to reduce their energy consumption and to propose new technologies.
This work is focusing on a hybrid system whose purpose is to estimate, by simulation, the daily output of a model with solar collector and heat exchanger in a typical sunny day.

II. PRESENTATION OF METHODS FOR DESALINATION

Figure 1 illustrates the desalination techniques classified into three broad categories: membrane processes, processes acting on the chemical bonds and processes being performed by phase change.
A method for separating salt water desalination in two parts: fresh water containing a low concentration of dissolved salts and concentrate brine. This process is energy-consuming. Various desalination techniques have been implemented over the years on the basis of the available energy [**5**].

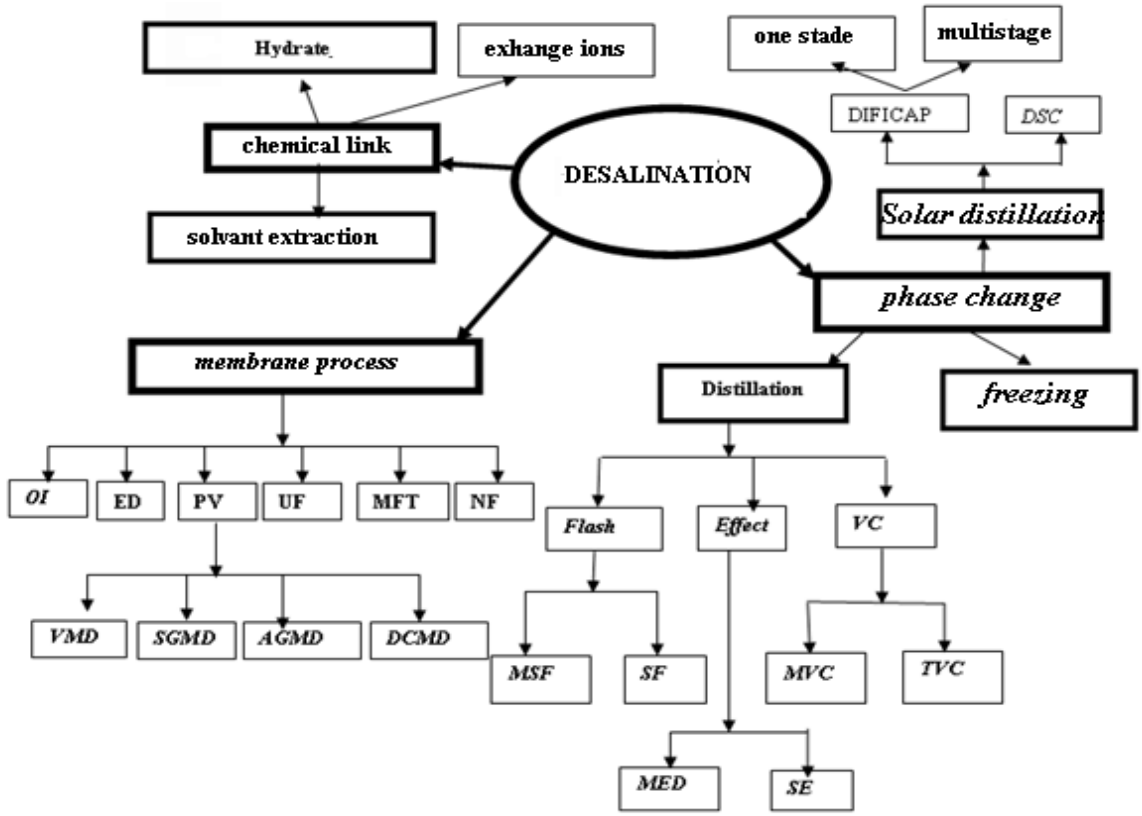

Figure 1 - Processes of desalination most used in the world

III. RENEWABLE ENERGY IN TECHNICAL AND DESALINATION

Renewable energy can come in extra desalination plants in different ways. Figure 2 shows the possible combinations. A desalination plant is likely to be independent in an area devoid of power grid. These systems are often hybrid, combining two or more sources of renewable energy. To ensure a continuous or semi-continuous operation regardless of weather conditions, autonomous systems are usually equipped with a storage device [2].

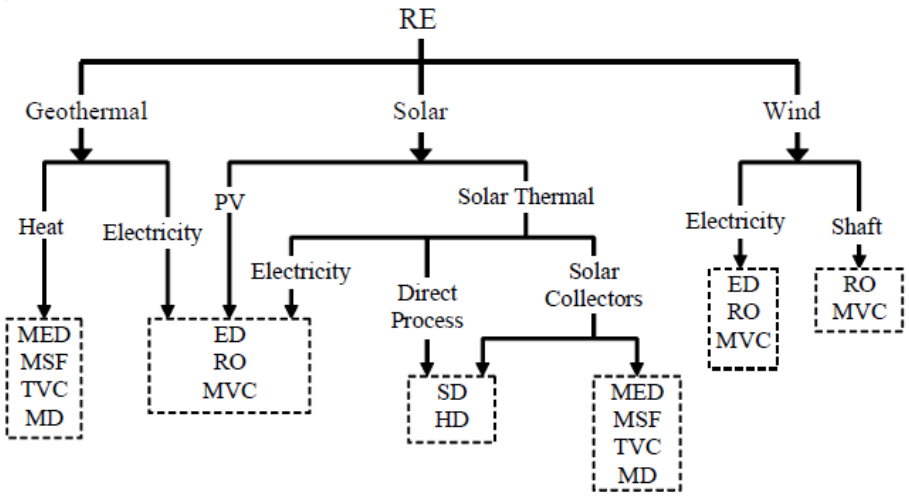

Figure 2 – Possible technological combinations in hybrid systems [2]

Table 1 provides an overview of recommended combinations according to input parameters, however, noticing that other combinations are also possible.

Table 1 - Combinations of desalination processes [**2**]

Feed Water quality	***Product water***	***resource available***	***System size***			***Suitable combination***
			Small (1-50) m^3/d	**Medium (50-100) m^3/d**	**Large (≥100 m^3/d)**	
Brackish water	Distillate	Solar	*			Solar distillation
	Potable	Solar	*			PV-RO
	Potable	Solar	*			PV-ED
	Potable	Wind	*	*		Wind-ED
seawater	Distillate	Solar				Solar distillation
	Distillate	Solar			*	Solar thermal-MED
	Potable	Solar				PV-RO
	potable	Wind	*			Wind-RO
	potable	Wind	*	*		PV-ED
	potable	Wind	*	*		Wind-MVC
	potable	Wind	*	*	*	Geothermal-MED
	potable	Geothermal		*	*	Geothermal-MED
	potable	Geothermal		*	*	

The general trend is to combine wind power solar thermal and geothermal technologies, with some membrane processes or phase changes. Some technologies (flash (MSF), successive multiple effect distillation (MED) and vapour compression (VC)) require energy-intensive feeding [5]. In countries where energy production is low a use-rate of that type of energy and desalination processes is available in the literature (Fig. 3).

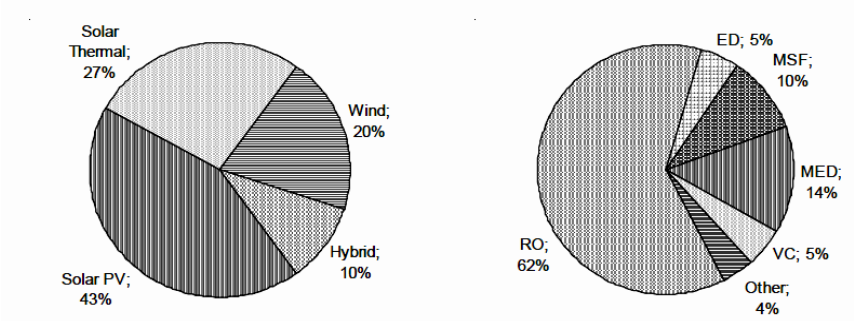

Figure 3 - Renewable energy-driven desalination processes and energy sources [2]

IV. DESCRIPTION OF HYBRID STILL

Our study applies to the process of membrane desalination type AGMD (Air Gap Membrane Distillation) which fluid flow is performed against the current. A schematic diagram of the desalination technology is shown in Figure 4. The salt-water supply is heated from a set (solar collector (7-8), conventional heat exchanger (5-6)). In the tubular porous membrane, the temperature of the brine is between 30 °C and 90 °C [**1**]. The wall of the tube is hydrophobic allowing only radial diffusion of the vapour. Steam generated through the membrane and the air gap condenses on the inner wall of the second pipe to be collected. Figure 5 illustrates flow directions through membrane.

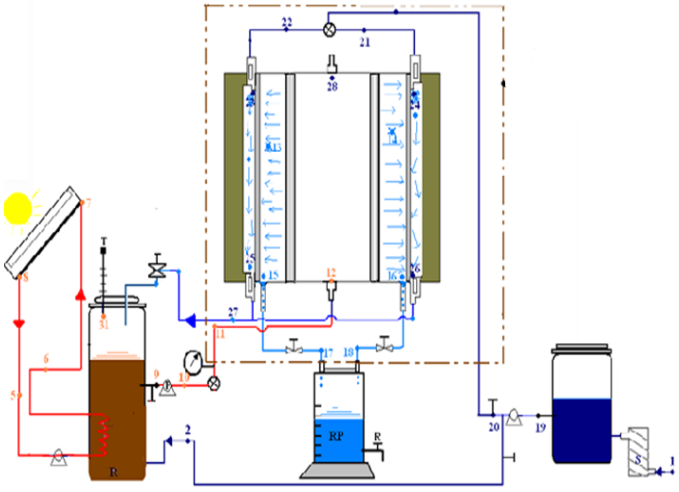

Figure 4 - Principle of operation of the AGMD

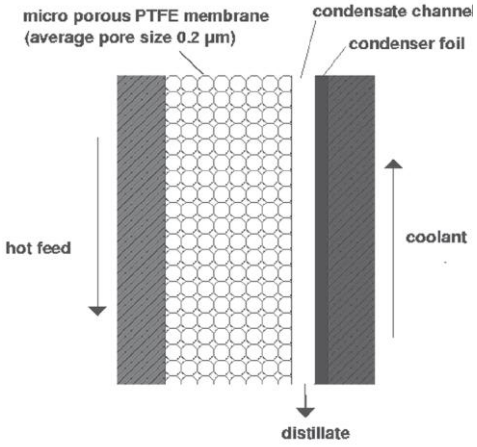

Figure 5 - Disposition and condensing the vapour through membrane

V. MODELING PROCESS AGMD

Assumptions:
- incompressible viscous non-Newtonian fluid,
- permanent and laminar regime,
- axisymetric flow,
- non-reactive membrane,
- uniform condensing temperature,
- isothermal flow.

5.1. Description of the flow patterns

Module freshwater producing uses the principle illustrated in Figure **6**. It consists of two concentric tubes. The inner tube is a hydrophobic membrane wherein a circulating hot salt solution and the outer tube is a condensation wall. Inside the wall of the condensing fresh water oozes while at the outside streamed cold water for cooling the wall.

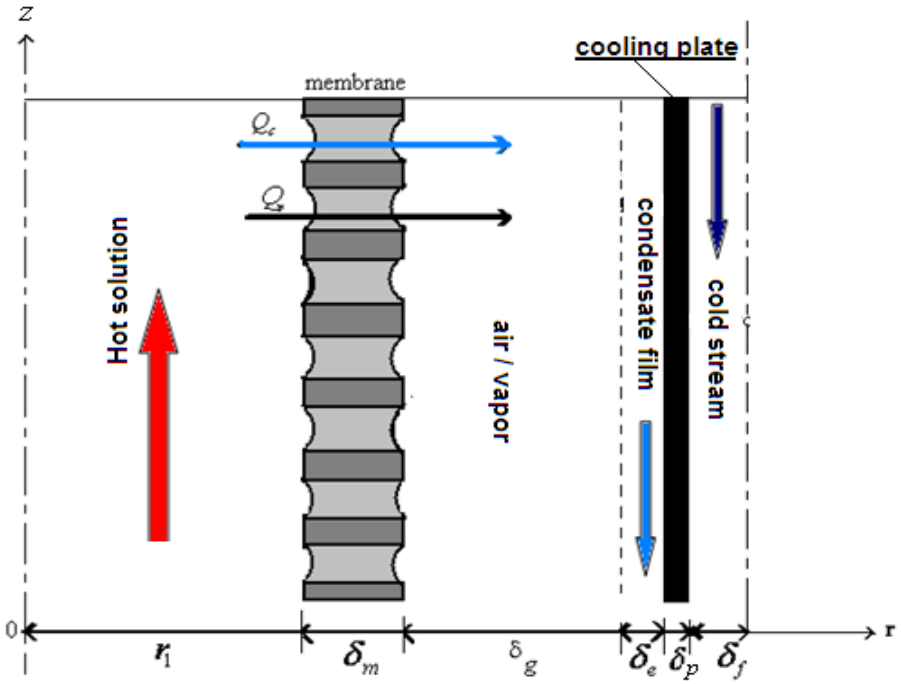

Figure 6 - Areas interfaces and flows

Legend- r_1: inner radius of the membrane; δ_m: thickness of the membrane; δ_g: thickness of air layer; δ_e: thickness of pure water; δp: wall thickness of condensation. δ_f: thickness of cold water runoff film .

5.2. Balance equations in the membrane

Boundary conditions

At the entrance of the membrane $z = 0$:

$$T(0,r,0) = T_e \quad (1)$$

At the outlet of the membrane $z = H_m$:

$$\left.\frac{\partial T}{\partial z}\right|_{(H_m,r,t)} = 0 \quad (2)$$

Along the axis of the membrane and for $r = 0$ and $0 \le z \le H_m$:

The slip condition at the wall where the heat flux exchange with the outside for (and) ($r = r_1$ and $0 \le z \le H_m$):

$$-k_h \left.\frac{dT}{dr}\right|_{(z,r_1,t)} = Q_c + Q_v \quad (4)$$

k_h: thermal conductivity of the hot solution, Q_c :heat flow unit due to conduction and Q_v : heat flow unit due to the steam.

5.2.1. Mass transfer through the membrane

The distiller is presented in the form of a double-tube heat exchanger and hydrophobic permeable wall. The three types of mechanisms called KMPT (Knudsen diffusion Molecular diffusion Poiseuille flow Transition) by which species of a gas mixture may

lose momentum in the movement – Knudsen flow, molecular diffusion of Fick or viscous diffusion.

5.2.2. Knudsen-Flow

This is a direct transfer of mass in the capillary wall, as a result of molecule-wall collisions. In the case of porous media, the vapour flow is given by:

$$J_K = \frac{2}{3}\frac{\varepsilon}{\tau} r_p \sqrt{\frac{8M_v}{\pi R_u \overline{T}_m}} \left(\frac{p_{hm} - p_{mg}}{\delta_m} \right) \quad (5)$$

With: $\overline{T}_m$ average temperature between the two sides of the membrane.

The membrane permeability due to Knudsen diffusion is given by the following expression:

$$K_{m,K} = \frac{2}{3}\frac{\varepsilon}{\tau}\frac{r_p}{\delta_m}\sqrt{\frac{8M_v}{\pi R_u \overline{T}_m}} \quad (6)$$

5.2.3. Molecular diffusion

Transfer to other species is due to collisions between pairs of different molecules. For a binary mixture (air and steam), the relationship of the diffuse flux through the membrane is obtained by Stefan's law [1] as

$$J_{m,S} = K_m . \Delta p_v \quad (7)$$

where J_m is diffusion flux of vapour through the membrane.

The permeability of the membrane due to molecular diffusion is defined by

$$K_m = \frac{\varepsilon P D_{v/a} M_v}{\tau \delta_m R_u p_a \overline{T}_m} \quad (8)$$

$$D_{v/a} = \frac{k_v}{\rho_v . C_{pv}} .$$

The average temperature of the membrane is given by the following equation:

$$\overline{T}_m = \frac{T_{mh} + T_{mg}}{2} \quad (9)$$

Moreover Qtaishat et al. [10] propose the term vapour / air quantity as a function of temperature:

$$PD_{v/a} = 1{,}985.10^{-5} T^{2{,}072} \quad (10)$$

The difference in partial pressure of saturated vapour of both sides of the membrane may be calculated from the law of Antoine [3] using the following equation:

$$\ln p_v = 23{,}328 - \frac{3841}{T - 45} \quad (11)$$

By replacing equation (10), equation (11) becomes

$$J_{m,S} = \frac{\varepsilon . PD_{v/a} M_v}{\tau \delta_m R_u \overline{T}_m} \left(\frac{p_{hm} - p_{mg}}{p_a} \right) \quad (12)$$

5.2.4. Viscous diffusion or Poiseuille

It is an indirect transfer to the capillary wall, this method starts with a transfer molecule-molecule collisions and terminating in a wall-molecule collision. The flow equation is:

$$J_p = \frac{1}{8\mu_g}\frac{r_p^2 \varepsilon}{\tau}\frac{M_v}{R_u \overline{T}_m}\frac{\Delta p_v}{\delta_m} \quad (13)$$

Or

$$J_p = K_p \Delta p_v \quad (14)$$

5.2.5. Exchanges of heat flow in a hybrid desalination system

The input saline solution (Fig. 7) is heated by a thermal system (heat exchanger hx) to an inlet temperature (T_{hx}, s). The water comes out at a temperature (T_{hx}, co) and enters a solar collector and sees its temperature to increase (T_{hi} = Te). The other side of the membrane, to the cooled (T_{ci}) allows water vapour to condense. This system is based heat exchange.

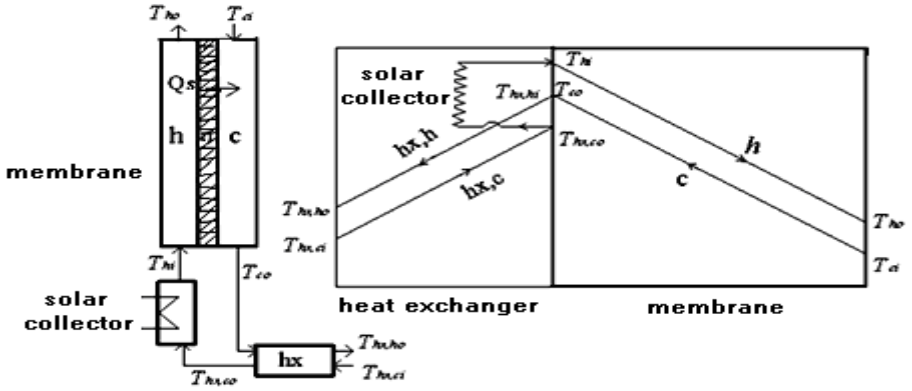

Figure 7 - Exchange of heat flow in a hybrid system

The total sensible heat flux (Q_s) is transferred from the hot surface of the membrane to the surface of condensation by two parallel modes. One is by conduction (Q_c) through the material of the membrane while the other mass transfer (Q_v):

$$Q_s = Q_c + Q_v \quad (16)$$

Accompanying the heat transfer the steam flow and heat transfer by conduction through the membrane are: The flow of heat by conduction (Q_c) is defined by:

$$Q_C = \frac{T_{hm} - T_{mg}}{R_m} = \frac{k_{cm}}{\delta_m}\left(T_{hm} - T_{mg}\right) \quad (17)$$

The latent heat flux (Q_v) of the vapour through the membrane is defined by:

$$Q_v = J_v.\Delta h_v \quad (18)$$

where Δh_v : enthalpy of unit mass of steam (J/kg)

The thermal conductivity of the membrane k_{cm} is defined by the equation (19) as:

$$k_{cm} = \varepsilon k_a + (1-\varepsilon) k_m \quad (19)$$

where

k_m: thermal conductivity of the material forming the membrane;

k_a: thermal conductivity of air

Thermal efficiency of the membrane is defined by the expression:

$$\eta_t = \frac{Q_v}{Q_s} \quad (20)$$

Temperatures of membrane interfaces/space of air, air/water and water/wall cooling space are given respectively by the relations (21), (22) and (13) as:

$$T_{mg} = \frac{R_s - R_m}{R_s} T_{hm} + \frac{R_m}{R_s} T_{pf} \quad (21)$$

$$T_{gd} = \frac{R_d + R_p}{R_s} T_{hm} + \frac{R_m + R_g}{R_s} T_{pf} \quad (22)$$

$$T_{dp} = \frac{R_p}{R_s} T_{hm} + \frac{R_s - R_p}{R_s} T_{pf} \quad (23)$$

The temperature of the hot vapour side of the membrane is expressed by the equation (24):

$$T_{hm} = \frac{h_h T_h - J_v \Delta h_v + \frac{k_{cm}}{\delta_m} T_{mg}}{h_h + \frac{k_{cm}}{\delta_m}} \quad (24)$$

The convection coefficient steady correlation is given by the Graetz-Leveque [3].

$$h_h = 1{,}86\left(R_e P_r \frac{d_h}{H_m}\right)^{0,33} \quad (25)$$

In dynamic mode, h_h is given by equation (26) as:

$$h_h = 0{,}116\left(R_e^{\frac{1}{3}} - 125\right) P_r^{\frac{1}{3}} \left[\frac{1 + \left(\frac{d_h}{H_m}\right)^{\frac{2}{3}}}{d_h}\right] \quad (26)$$

The temperature at the boundary *air*/condensate is expressed by equation (27):

$$T_{gf} = T_{mg} + \frac{\delta_g}{k_g}\left(J_v \Delta h_v - h_h\left(T_h - T_{hm}\right)\right) \quad (27)$$

The temperature at the boundary condensate *a*/cold wall is expressed by equation (28):

$$T_{fp} = T_{gf} + \frac{h_h}{h_f}\left(T_{hm} - T_h\right) \quad (28)$$

The temperature at the wall can be defined as:

$$T_p = T_{amb} + \frac{h_h}{h_{xt}}\left(T_h - T_{hm}\right) \quad (29)$$

VI. RESULTS AND DISCUSSION

Figure 8 illustrates the evolution of the polarization coefficient of the temperature between the inlet and outlet of the tube, and for various porosities

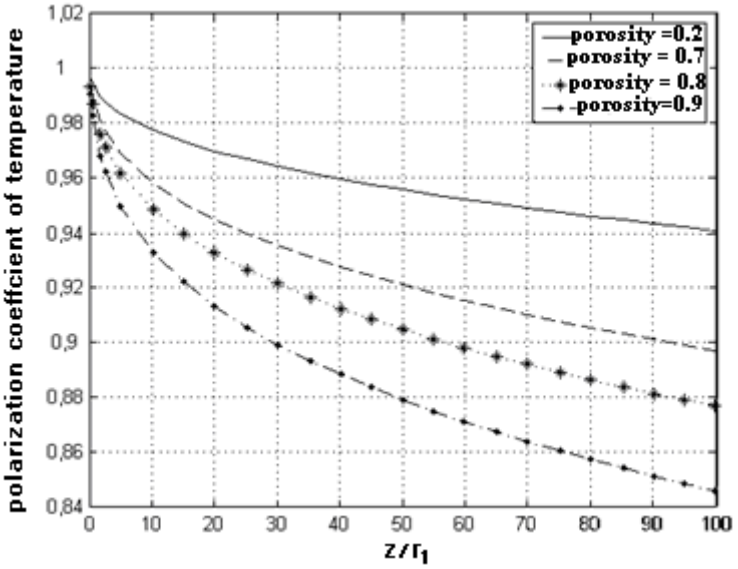

Figure 8 - Evolution of the polarization coefficient of the temperature for various porosities

This coefficient is found to decrease from the inlet to the outlet of the tube, also by increasing the porosity. Polarization temperature causes a significant loss of the driving force for transport ($T_{hm} - T_{gf}$) compared to the imposed force ($T_f - T_c$). This force is also reduced by the pressure drop of water vapour supply side due to the presence of salt. A validation of the theoretical model was performed by comparing our results with the experimental results of Banat [13] on a membrane.

The results reported by Baoan Li [11] and Z. Ding [12] indicated a value of the polarization coefficient equal about 1.0 was acceptable, which is a good agreement with our results.

Moreover, our theoretical model can be validated by the results reported by Banat [13] (Fig.9)

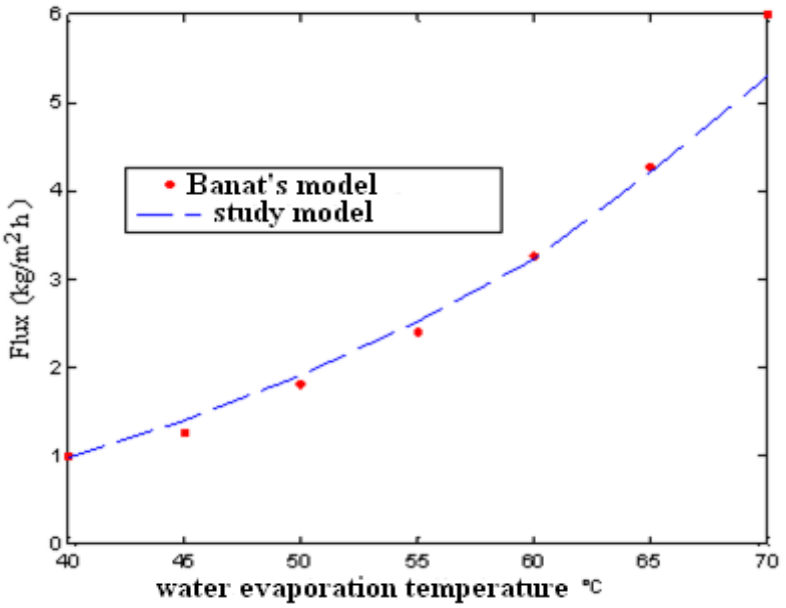

Figure 9 - Comparison of the model with the experimental values of Banat [13]

We will determine which one among the two heats (by conduction or vapour transfers) that dominates over. For this we set the input data: k_m= 0.05 $W.m^{-1}K^{-1}$,, $\delta m = 4.10^{-4}$ m, Tc = 20 °C. Figure 10 shows the effect of the temperature of the hot salt solution on the process of heat transfer through the membrane module while Figure 11 exhibits the evolution of the power unit due to thermal conduction.

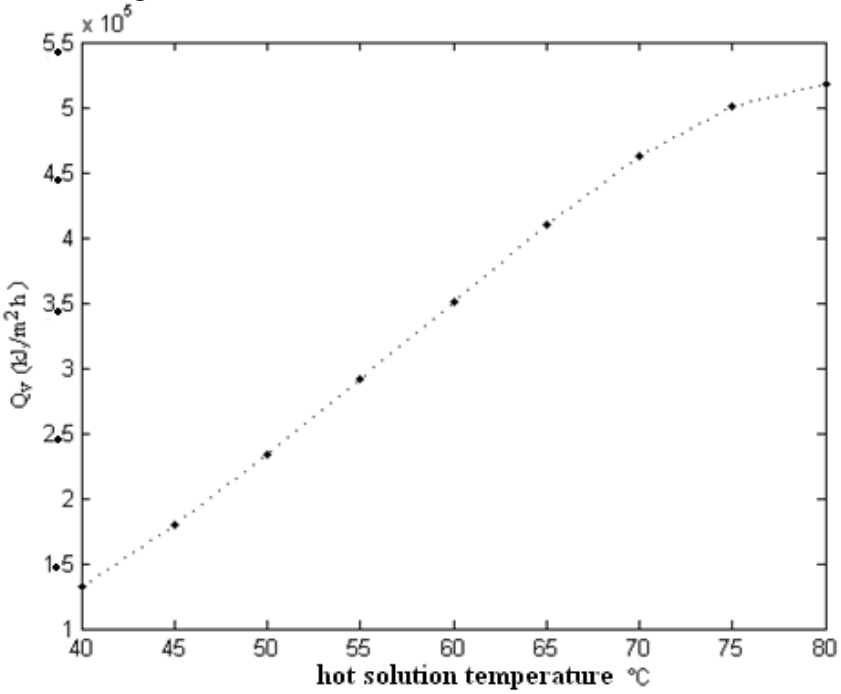

Figure 10 - Evolution of the unit thermal power due to the flow of steam

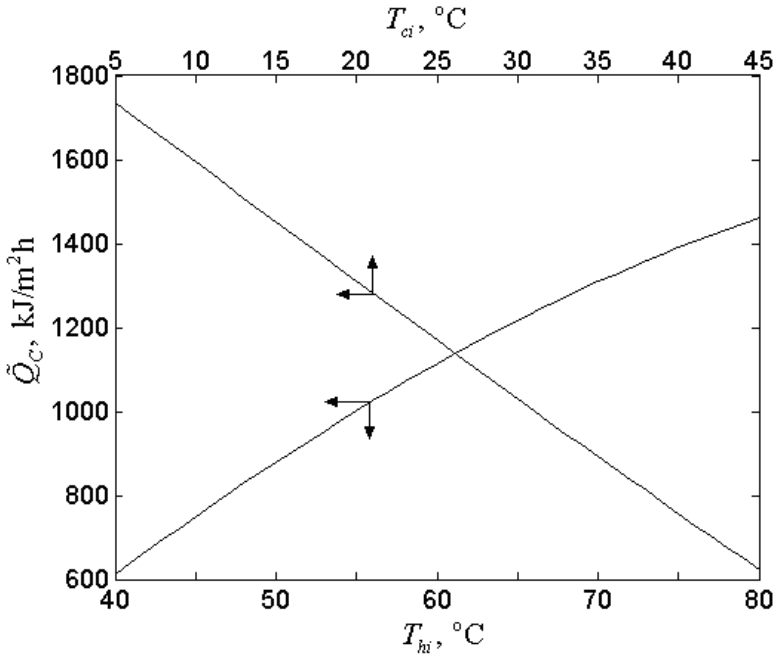

Figure 11 - Evolution of the power unit caused by conduction

For a variation of the temperature of 40 °C to 80 °C, heat due to conduction augment about 8 % than that due to vapour transport. But taken as a whole, we observe that heat due to transportation is 69 times greater than that due to conduction. So in the process of transport across the membrane modules, the heat flux due to conduction is found to be relatively low. Under the same conditions as above, we consider here the production of water per hour.

The efficiency of the membrane process has been assessed (Fig. 12). This figure exhibits the evolution of the efficiency of the process according to the hot salt water temperature for the system power.

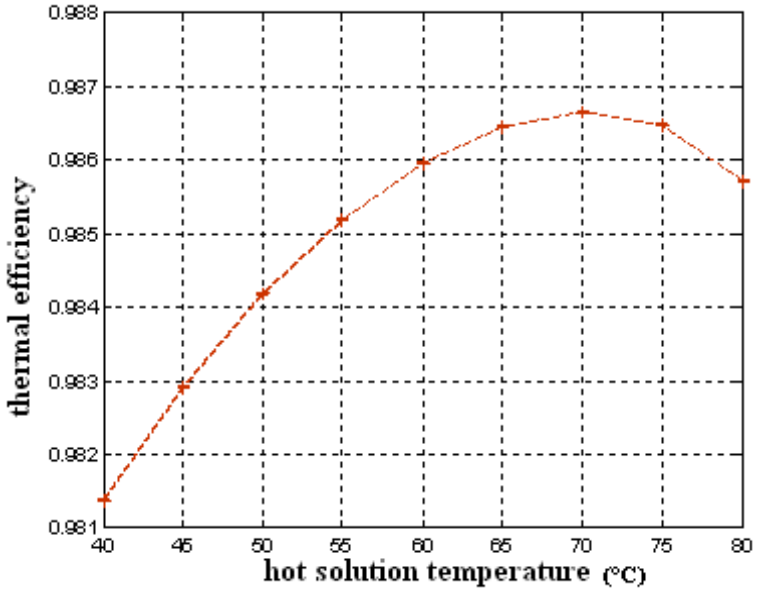

Figure 12 – Thermal efficiency as a function of the temperature of the hot solution.

Figure 13 illustrates the influence of temperature on the production of fresh water (for H_m = 0.2 m and r_1 = 2 mm

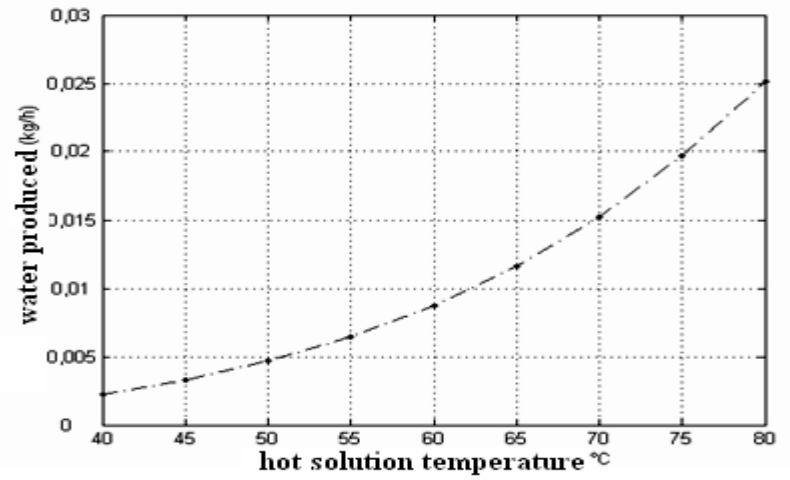

Figure 13 - Effect of temperature on distillate production for input data

Figure 14 shows the temporary change in temperature for a hot typical day. Changes in daily temperature when using solar system describes a bell curve (Fig. 14), whose peak is observed at 14 h. The same is true for the flow of water vapour (Fig. 15) and brine (Fig. 16). This time corresponds to the sunshine hour, the reference sunny day, at which the sunlight rate is found to be highest in the study area.

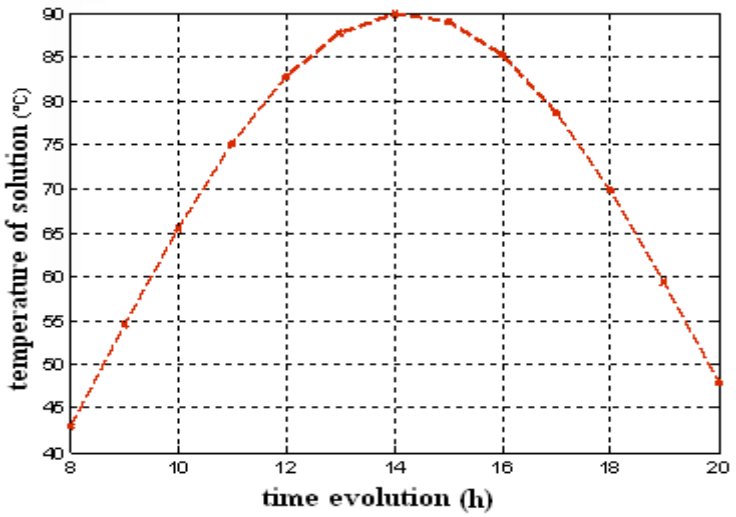

Figure 14 - Evolution of daytime temperature of the hot solution produced by solar

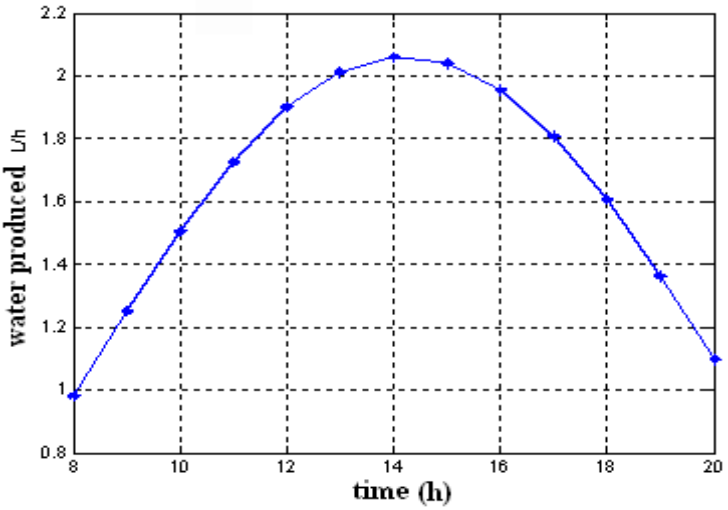

Figure 15 - Evolution of the daily flow of water vapour through the membrane

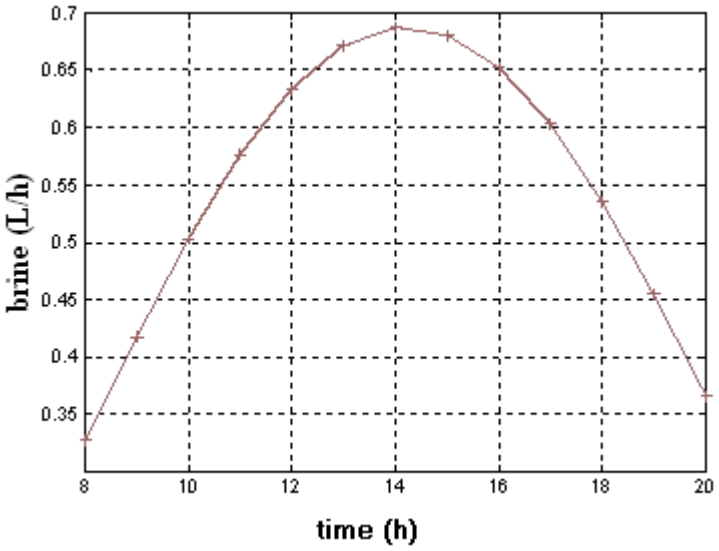

Figure 16 - Evolution of the brine flow in the membrane

Figure 16 illustrates in fact, the production of distilled water in the membrane depending on the temperature of the hot water solution, the maximum quantity being produced at 14 h when solar system was used.

Figure 17 exhibits the daily fresh water changes with the temperature of the hot solution production for such a sunny day.

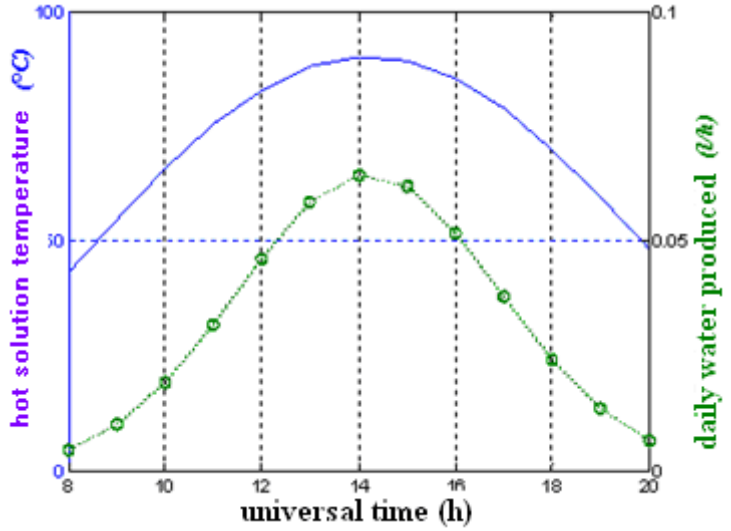

Figure 17 - Changes in temperature and production during a typical sunny day.

For a sunny day, the highest temperatures generated by the solar collector are observed between 11 h 30 and 16 h 30 when using solar system.
In Figure 18 we can observe the evolution of the production of fresh water according to the temperature of the hot solution for the input data. We can easily observe the fresh water production increases with increasing hot water temperature, which is not a surprise.

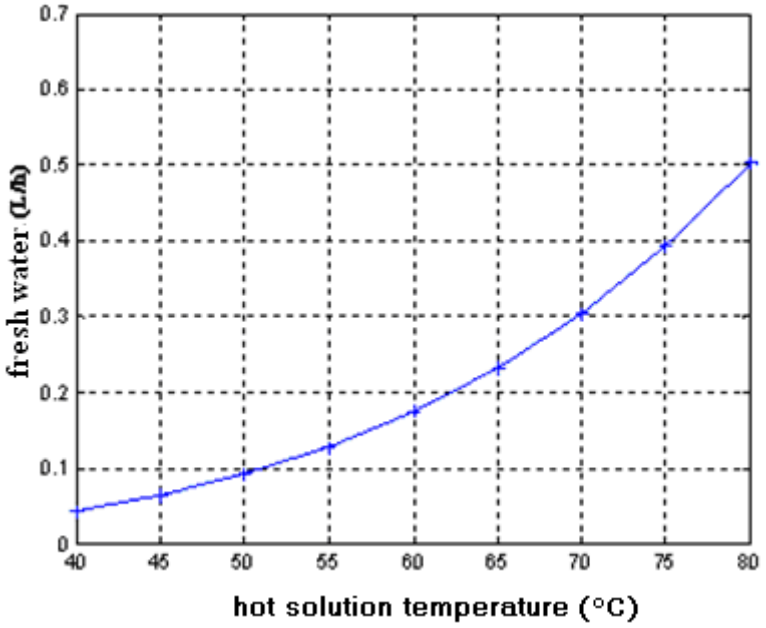

Figure 18 - Fresh water production depending on the temperature of the input data

VII. CONCLUSION

Modelling as the simulation allowed us to determine the flow phenomena in a hybrid membrane module. The characteristics of the process (AGMD) simulated dynamic system gave acceptable results on the flow of water vapour and thermal efficiency. The significant information that we can draw from this work, are listed as follows.

• The input temperature of the saline solution appear to be a significant factor on the flow of the permeated vapour but it is found to have a lesser effect on the thermal efficiency of the process manner.

• On the other hand, low cooling temperatures is shown to improve the flow of steam with decreasing the thermal efficiency of the process

• The steam flow through the membrane increases rapidly with the temperature of the feed solution.

• Finally, a study on heat transfer permits us to observe that the thermal energy mass transfer dominates over thermal conduction. And this is from the modelling of these discussions we determined the daily production and the system efficiency.

LIST OF SYMBOLS

C_s	mole fraction of NaCl
C_{pv}	vapour mass thermal capacity at constant pressure, $J.kg^{-1}.K^{-1}$
d_h	half-width of the flow channel, m
D_s	salt diffusion efficiency, $m^2.s^{-1}$
g	gravitational acceleration, $m.s^{-2}$
h	specific enthalpy, $J.kg^{-1}$
H	membrane length, m
J	length-averaged permeate flux at the hot side of the membrane, $kg.m^{-2}.s^{-1}$
J_v	local permeate flux at the hot side of membrane, in vapour phase, $kg.m^{-2}.s^{-1}$
k	thermal conductivity, $W.m^{-1}.K^{-1}$
K	membrane permeability, $m^{-1}.s$
M	molar mass, $kg.mol^{-1}$
$\dot{m}$	mass flow rate, $kg.s^{-1}$
Nu	Nusselt number
P	pressure, Pa
Pr	Prandlt number
P_v	water vapour pressure, Pa
Q	unit area rate of heat transfer, $J.m^{-2}.s^{-1}$
R_e	Reynolds number of the hot solution channel
R_u	gas law constant, $J.kmol^{-1}.K^{-1}$
r_p	membrane pore size, m
r_1	largest membrane pore , m
T	temperature, ^oC
T_{ci}	inlet temperature of cold solution, ^oC
T_{hi}	inlet temperature of hot solution, ^oC
$\bar{T}$	Average temperature, ^oC
V	velocity, $m.s^{-1}$
V_e	velocity of feed solution, $m.s^{-1}$
Vr	the velocity in radius direction, $m.s^{-1}$
r	coordinate normal to the solution flow
z	coordinate along the solution flow

Greek letters

ΔP	water vapour pressure difference, Pa
δ	Thickness or width, m
ε	porosity of the membrane
γ_l	surface tension of water, $N.m^{-1}$
μ	dynamic viscosity, $kg.m^{-1}.s^{-1}$
ρ	density, $kg.m^{-3}$
τ	tortuosity

Subscripts

a	Air
atm	Atmosphere
Avg	Average
c	cold solution
f	condensate film

fp	condensate film/cooling plate interface
g	vapour/air gap
gf	air gap/condensate film interface
h	hot solution
hi	inlet of the hot channel
hm	hot liquid/membrane interface
i	inlet of the channel or ith domain
m	membrane
mc	membrane cold side
mg	membrane/air gap interface
p	cooling plate
pc	cooling plate/cold channel interface
s	solution
v	vapour

REFERENCES

[1] ALKLAIBI. A. M, LIOR. N: Membrane-distillation desalination: Status and potential, *Desalination, 171, pp.111-131, 2005*.

[2] E. MATHIOULAKIS, V. BELESSIOTIS, E. DELYANNIS - *Desalination by using alternative energy* - Review and state-of-the-art National Center for Scientific Research (NCSR) "Demokritos", Aghia Paraskevi, 153-10, Athens, Greece, 2006

[3] M.SENE, –Transferts de chaleur et de masse dans des procédés de dessalement par distillation membranaire, type AGMD.valorisation des ressources en eau dans le delta du saloum – Thèse de doctorat, Université Cheikh Anta Diop de Dakar Sénégal (2010).

[4] AKILI D. K, IBRAHIM K. K, Jong-Mihn WIE – *Advances in seawater desalination technologies* – Royal Commission for Jubail & Yanbu, Saudi Arabia.

[5] Nizar LOUSSIF, Jamel ORFI, Moussa SENE, Ousmane SOW, Thierry MARE, Mamadou ADJ – *Transferts couplés de chaleur et de masse dans une unité de dessalement par distillation membranaire* – Université de Monastir, Tunisie, King Saud University, Riyadh, KSA, Université Cheikh Anta Diop de Dakar, Sénégal, IUT St Malo, France

[6] E. DELYANNIS and V. BELESSIOTIS – *A historical overview of renewable energies* – Proc. Mediterranean, Conference on Renewable Energy Sources for Water Production, Santorini, Greece, 10–12 June 1996, EURORED network, CRES, EDS, 1996, pp.13–17.

[7] G.F. LEITNER – *Is there a water crisis* – Int. Desalination and Water Reuse Quart. 7(4) (1998) 10–21.

[8] E.D. HOWE – *Fundamentals of Water Desalination* – Marcel Dekker, New York, 1974.

[9] M. Khayet, M.P. Godino, J.I. Mengual, Nature of flow on sweeping gas membrane distillation, J. Membr. Sci. 170 (2000) 243–255.

[10] M. QTSAISHAT, M. MATSUURA, B. KRUCZEK, M. KHAYET, – *Heat and mass transfer analysis in direct contact membrane distillation* – Industrial Membrane Research Centre, Department of Chemical Engineering, University of Ottawa Desalination 219 (2008) 272-292

[11] BAOAN LI, KAMALESH, K. SIRKAR – *Novel membrane and device for vacuum membrane distillation-based desalination process* – Journal of Membrane Science 257 (2005) 60-75.

[12] Z. DING, R. MA, A.G. FANE – *A new model for mass transfer in direct contact membrane distillation* – Centre for Membrane Science and Technology, School of Chemical Engineering and Industrial Chemistry, University of New South Wales, Sydney 2052, Australia, Desalination 151 (2002) 217-227.

[13] F. A. BANAT – *Membrane distillation for desalination and removal of volatile organic compounds from water* – Ph,D. thesis, McGill University, Canada, (1994).